ORIGINAL PAPER

Enhancement on amorphous phase in solid biopolymer electrolyte based alginate doped NH$_4$NO$_3$

N. M. J. Rasali[1] · Y. Nagao[2] · A. S. Samsudin[1]

Abstract

The present work deals with the development of solid biopolymer electrolyte (SBE) system using a promising biopolymer, namely, alginate doped with various amount of ammonium nitrate (NH$_4$NO$_3$). The SBE system has been successfully prepared via the solution-casting method. The Fourier transform infrared (FTIR) analysis carried out suggests that interaction has occurred between alginate and NH$_4$NO$_3$ via COO$^-$. The X-ray diffraction analysis (XRD) also discloses that the addition of NH$_4$NO$_3$ affects the alginate SBE system by reducing the crystallinity and transforming it to an amorphous phase. The ionic conductivity of SBE system has been measured using electrical impedance spectroscopy (EIS), and it was found to achieve a maximum value of 5.56×10^{-5} S cm^{-1} at ambient temperature (303 K) for a sample containing 25 wt.% NH$_4$NO$_3$. The SBE system was found to obey the Arrhenius behavior where the system is thermally activated, and the differential scanning calorimetry (DSC) analysis demonstrated the decreased in glass transition temperature (T_g) upon the addition of the dopant. The mobility (μ) and diffusion coefficient (D) were found to affect the ionic conductivity trend as observed via IR-deconvolution approach. The alginate–NH$_4$NO$_3$ SBE sample with the highest conductivity has a transference number t_{ion} of 0.97 which further indicates that the conduction species is a cation.

Keywords Polymer electrolytes · Amorphous phase · Ionic conductivity · Deconvolution approach

Introduction

Owing to the increasing nature of industrial applications that require a reasonable energy storage capacity as well as source, primarily for electrochemical devices, due attention has been given towards the development of such power source [1–5]. Liquid electrolytes (LE) are extensively used for electrochemical devices rather than other forms of electrolytes due to its high ionic conductivity properties [6, 7]. Previous studies with regard to LE revealed other desirable properties, such as good thermal stability low toxicity [8–10]. However, it is worth noting that there are also undesirable issues associated with LE that has been reported in the literature, namely, leakage, poor electrochemical stability, and corrosion reactions with electrode [11]. These

drawbacks have somewhat render LE less attractive for electrochemical devices. Solid biopolymer electrolytes (SBEs) have been demonstrated to be a viable promising alternative to LE. SBEs are the formation of salt dispersed in a polymer matrix into an ion conducting system. The salt mainly supplies mobile ions while the polymer host acts as a solvent in SBEs. The potential application of SBEs have been recognized due to its low energy density properties, ease of preparation, lightweight, leakage free, and excellent mechanical properties [12–15].

There are a number of renewable biopolymer-based resources that are suitable as host polymers, such as starch [16], chitosan [17], hydroxyethyl cellulose [18], and agarose [19, 20] amongst others. Alginate is a linear polysaccharide that comes from the family of carbohydrates as shown in Fig. 1 [21], which is a derivation of brown algae, and it is a natural polymer that is water soluble [22, 23]. Chemically, alginate is made up of β-D-mannuronic acid and α-l-guluronic acid monomers [24, 25] and it has gained due attention primarily due to its low cost, biocompatibility, highly hydrophilic, and not toxic [26–28]. Therefore, owing to the aforesaid properties, this particular natural polymer has the potential of becoming a promising candidate for renewable-based polymer electrolytes.

✉ A. S. Samsudin
    ahmadsalihin@ump.edu.my

1   Advanced Materials Group, Faculty of Industrial Sciences and Technology, Universiti Malaysia Pahang, 26300 Gambang, Pahang, Malaysia

2   Japan Advanced Institute of Science and Technology, School of Materials Science, 1-1 Asahidai, Nomi, Ishikawa 923-1292, Japan
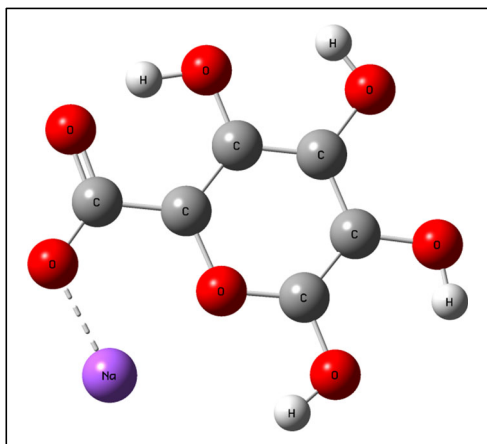
Fig. 1 Optimized molecular structure of alginate retrieved from the Gaussian software

Table 1 Designation of the alginate-ammonium nitrate

Composition of NH$_4$NO$_3$ (wt.%)	Designation
0	S0
5	S1
10	S2
15	S3
20	S4
25	S5
30	S6
35	S7

As such, this work focuses on the potential of alginate as the polymer host and ammonium nitrate as the ionic dopant. It is worth noting that ammonium salt is believed to be an excellent proton donor. The transportation of ions of the developed system is also investigated to evaluate to what extent does the ionic conductivity enhancement it yields against other systems developed [29, 30]. To the best of the authors' knowledge, the present investigation is novel. The present system is characterized by using Fourier transform infrared (FTIR) spectroscopy, X-ray diffraction (XRD), electrical impedance spectroscopy (EIS), transference number measurement (TNM), and differential scanning calorimetry (DSC) respectively.

Material and methods

Sample preparation of SBE thin film

Approximately, 2 g of alginate (Sigma-Aldrich Co.; MW 12,000–40,000) was dissolved into distilled water. Then, different amounts of NH$_4$NO$_3$ (5–35 wt.%) was added into the alginate solution, and the solution was stirred until it becomes homogeneous. The homogenous solution of alginate–NH$_4$NO$_3$ was cast into a petri dish and was left to dry at room temperature to obtain the alginate–NH$_4$NO$_3$ films. The designation of the samples is shown in Table 1.

Characterization of SBE thin film

Fourier transform infrared spectroscopy

The complexation of the sodium alginate and ammonium nitrate is examined via Perkin Elmer 100 attenuated total reflection (ATR) FTIR spectroscopy with germanium crystal. The sample was placed on germanium crystal,

and the infrared light was passed through the sample within the frequency range from 4000 to 700 cm^{-1} with a resolution of 2 cm^{-1}.

X-ray diffraction

The XRD pattern of alginate–NH$_4$NO$_3$ SBE system was performed by using a Rigaku MiniFlex II diffractometer. The sample was cut into a suitable size and then placed onto a glass slide. The spectra of XRD scanned were fixed at 2θ between 5° and 80° using CuKα as the radiation source. The crystallite size (D) analysis was carried out via the full width half maximum (FWHM) information. The calculation is based on the Debye-Scherrer equation as shown below [31, 32]:

$$D = \frac{K\lambda}{\text{FWHM}\cos\theta} \tag{1}$$

where $K = 0.94$, $\lambda = 0.154$ nm, and $\theta =$ peak location.

Electrical impedance spectroscopy

Ionic conductivity of SBE system was characterized by using HIOKI 3532-50 LCR Hi–Tester at an ambient temperature of 343 K with a frequency range from 50 Hz to 1 MHz. The ionic conductivity, σ, of the electrolyte was measured using the following equation:

$$\sigma = \frac{t}{R_b A} \tag{2}$$

where t is the thickness of the electrolytes, R_b is the bulk resistance which was obtained from the plot of imaginary impedance (Z_i) versus real impedance part (Z_r), and A is the electrode-electrolyte contact area (cm^2).

FTIR deconvolution

The FTIR deconvolution analysis was carried out via the Origin Lab 8.0 software. The area under the peak was

determined, and the free ions (%) were calculated using the equation as follows [33–36]:

$$\text{Percentage of free ions } (\%) = \left(\frac{A_f}{A_f + A_c}\right) \times 100\% \quad (3)$$

where A_f is the area under the of the free ions region, while A_c is the total area under the peak of the contact ions. The number (η), mobility (μ), and the diffusion coefficient (D) of the mobile ions are determined by using the following equations [33–37]:

$$\eta = \left(\frac{MN_A}{V_{total}}\right) \times \text{free ions } (\%) \quad (4)$$

$$\mu = \frac{\sigma}{\eta e} \quad (5)$$
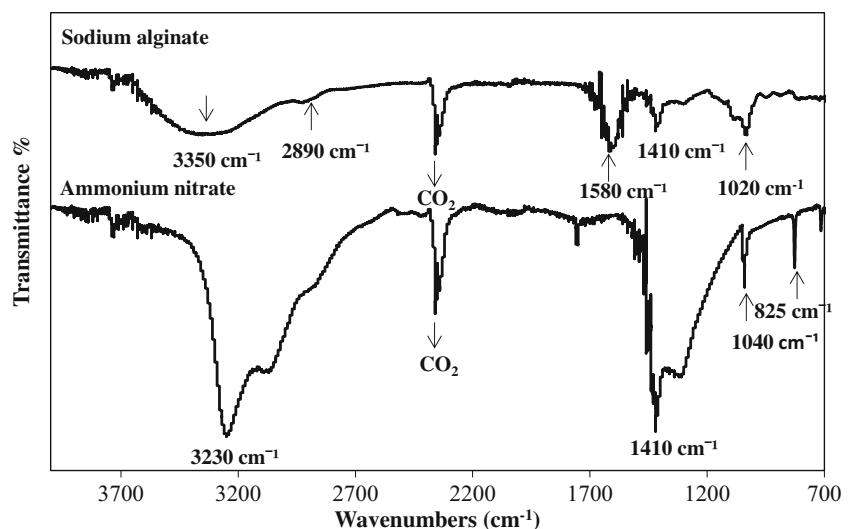
$$D = \left(\frac{kT\mu}{e}\right) \quad (6)$$

In this work, M is the number of moles of the salt based on weight percentage, N_A is Avogadro's number, and V_{total} is the total volume of the SBE system, while e is the electric charge, k is the Boltzmann constant, and T is the absolute temperature in Kelvin.

Transference number measurement

Transference number measurement (TNM) was measured using a direct current (DC) polarization technique [38, 39] to evaluate the quality of the ionic conduction. The DC value was monitored as a function of time by using a cell potential of 1.5 V across the sample sandwiched between two stainless steel electrodes. To calculate the ionic transference, t_{ion} value, the following equation is employed [40]:

$$t_{ion} = (I_i - I_s)/I_i \quad (7)$$

$$t_{ele} = (I_s/I_i) \quad (8)$$

where I_i and I_s are the total and residual currents, respectively.

Differential scanning calorimetry

The thermal properties of this work were determined through a NETZSCH5 differential scanning calorimetry (DSC). The glass transition temperature (T_g) of the different SBE sample (4 mg) was measured at a heating scan rate of 10 °C/min from 30 to 550 °C.

Results and discussion

FTIR analysis

The FTIR analysis evaluates the complexation between the host polymer and the salt. This analysis is non-trivial to further understand the conduction mechanism of the proposed SBE system. The IR spectrum of pure alginate and ammonium salt is presented in Fig. 2, and their functional groups are tabulated in Table 2.

The primary bands that exist with the coordinating site (oxygen) in alginate are the stretching of COO^-, –OH, and C–O–C bending. These bands are demonstrated to be significant and are highlighted if any changes of peaks occur in these functional groups. The molecular structure of alginate is quite similar to carboxymethyl cellulose (CMC) as the only difference between them is the presence of the carboxymethyl group on CMC as reported by other researchers [49, 50].

The functional groups of interest for the SBE which represent the complexes of alginate–NH_4NO_3 are highlighted in Fig. 3. Based on Fig. 3, it shows that the FTIR spectrum of alginate-ammonium nitrate SBEs that are defined at peaks


Fig. 2 The IR spectrum of powder of alginate and pure ammonium salt

Table 2 List of band modes of alginate-ammonium nitrate

Material	Wavenumber (cm^{-1})	Assignment	References
Alginate	1020	C-O-C	[41]
			[42]
			[43]
	1580 and 1410	COO$^-$ stretching	[44]
			[45]
			[42]
	2890	C–H stretching	[44]
			[45]
			[42]
	3350	O–H stretching	[44]
			[45]
			[42]
	1040	Symmetric stretching (NO$_3^-$)	[46]
			[47]
			[48]
	1410	Asymmetric stretching (NH$_4^+$)	[46]
			[47]
			[48]
	3230	Asymmetric stretching mode (NH$_4^+$)	[46]
			[47]
			[48]

1415 and 1598 cm^{-1} corresponds to the present of COO$^-$ stretching of carboxylate anion of (C=O) and (C–O$^-$) in alginate, respectively [43, 45, 51]. The absorption by carbon dioxide (CO$_2$) may be observed with a sharp peak between 2200 and 2700 cm^{-1}. It is evident from Fig. 3a that the intensity of the peak at 1598 cm^{-1} was found to increase with the addition of the NH$_4$NO$_3$. It is also observed that only a slight change in the wavenumber of 7 cm^{-1} resolution. Meanwhile, the peak at

Fig. 3 **a** FTIR spectrum between 1500 and 1800 cm^{-1}, **b** FTIR spectrum between 1200 and 1500 cm^{-1}, **c** FTIR spectrum between 900 and 1200 cm^{-1}, and **d** FTIR spectrum between 3000 and 3700 cm^{-1}
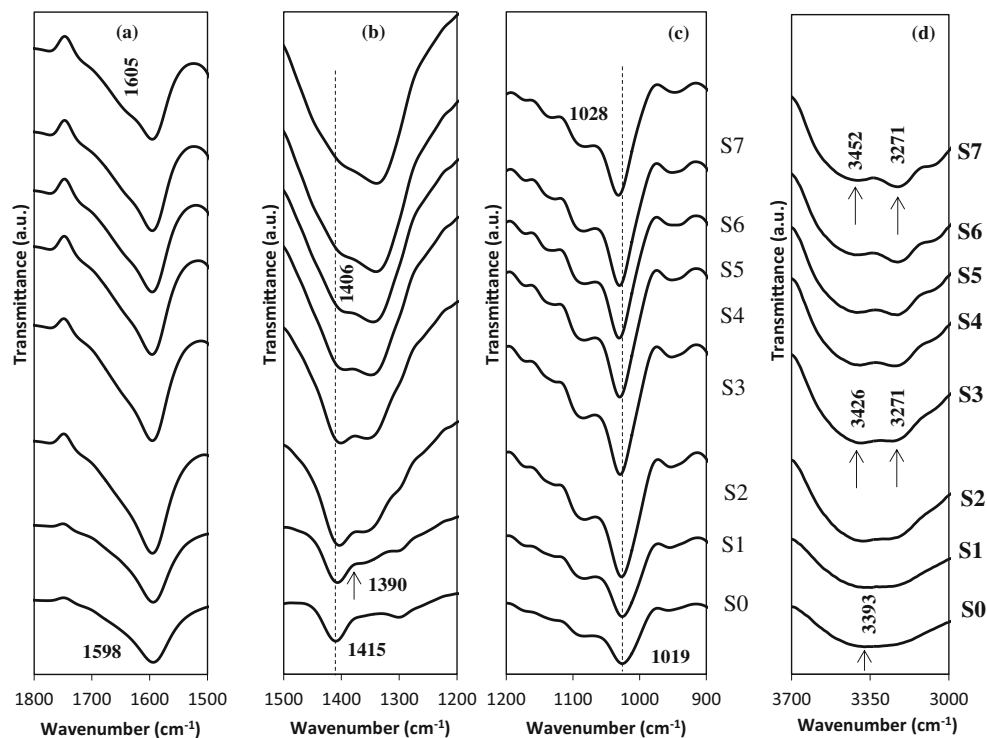
wavenumber 1415 cm^{-1} is found to shift to a lower wavenumber (1406 cm^{-1}) upon the addition of 25 wt.% NH$_4$NO$_3$ and disappears beyond the value. These apparent changes are expected at this functional group, primarily due to the coordination interaction between (COO$^-$) in the alginate with H$^+$ of [NH$_4^+$] substructure in NH$_4$NO$_3$ which reflects the protonation (either by C–O$^-$···H$^+$NH$_3^+$ or C=O···H$^+$NH$_3^+$).

It was observed that the increase of NH$_4$NO$_3$ composition in alginate resulted in a higher concentration of H$^+$. Accordingly, more ions are inhibited towards the alginate via (COO$^-$) to form hydrogen bonding, and this phenomenon is demonstrated through the shifting of peak to the lower wavenumber. This phenomenon has also been reported in previous studies [35, 52] where the authors' believed that the H$^+$ ion that originated from the ammonium salts acts as a conducting ion which migrates towards the anion group in polymer electrolyte system. The conduction takes place through the Grotthus mechanism when there is an electric field applied, and this is related to the exchange of ions between complexed sites, suggesting that complexation has taken place between the biopolymer and ionic dopant. The disappearance of the peak at ~ 1415 cm^{-1} could be either due to the higher composition of NH$_4$NO$_3$ that did not associate or the ions that recombine to form neutral ion pairs. A similar observation was made by Mason et al. [53] and Kadir et al. [54] in their respective works. A new peak was observed at 1390 cm^{-1} in the entire SBE system, and this can be attributed to the existence of NH$_4^+$ from NH$_4$NO$_3$. The interaction consequently results in the increase of relative intensity due to the increment of the NH$_4$NO$_3$ composition. These occurrences could be attributed to the coordination of NH$_4^+$ ions with the polar group present in the alginate group when NH$_4$NO$_3$ was introduced into the system. Other researchers [55, 56] that utilize ammonium salts as a dopant in polymer electrolyte system also observed similar behavior. The authors opined that the new peak that appears at wavenumber ~ 1400 cm^{-1} corresponds to the NH$_4^+$ ions of the ammonium salts.

Another evidence to further suggest that the complexation has taken place is noticeable at wavenumber 1019 cm^{-1} (C–O–C of alginate) which was observed to shift to a higher wavenumber (1028 cm^{-1}) when NH$_4$NO$_3$ was added in the present system. The changes of IR peak in this region can be due to the migration of NH$_4^+$ towards C–O–C. There are strong contributions of hydrogen bonding and coordination interaction of H$^+$ to the C–O–C between alginate and NH$_4$NO$_3$ as found in other similar systems using ammonium salts [54]. There are two possible charge carrier components in the polymer–salt electrolyte systems either cation or anion [55] and this can be demonstrated from transference number measurement analysis. Based on previous reports [56, 57], it is believed that H$^+$ is the only cation that contributes towards the

ionic transport properties, and this further establishes that the entire event occurred at coordinating site (oxygen) of the host biopolymer (alginate).

On the other hand, it can be seen that –OH stretching transpired at wavenumber 3393 cm^{-1} for the un-doped SBE system. It could be seen that with the addition of NH$_4$NO$_3$ in SBE system, a broad absorption peak of OH stretching at 3393 cm^{-1} is shifted to a higher wavenumber of 3452 cm^{-1}. A new peak was observed at 3271 cm^{-1} with the addition of 15 wt.% NH$_4$NO$_3$, and this could be attributed due to the presence of asymmetrical N–H stretching from NH$_4$NO$_3$. In addition, there is an overlapping of peaks observed in the –OH region which leads to the shifting of –OH group in alginate when NH$_4$NO$_3$ was introduced. This event is found to be similar as observed by other researchers who utilized NH$_4$NO$_3$ as an ionic dopant in polymer electrolyte system [47, 49]. Table 3 summarizes the changes in the wavenumber where it is believed that complexation has occurred between alginate and NH$_4$NO$_3$ in SBE system.

XRD analysis

The XRD patterns of solid biopolymer electrolyte (SBE)-based alginate with different composition of NH$_4$NO$_3$ are shown in Fig. 4. In the present system, the addition of NH$_4$NO$_3$ is expected to assist the biopolymer host in enhancing the amorphous phase in the SBE system [61]. Based on Fig. 4, the semi-crystalline hump was found at ~ 13°, ~ 21°, and ~ 38° for sample S0, which corresponds to the un-doped sample. Previous research report that the pure alginate powder consists of two main semi-crystalline peaks which can be found at $2\theta = 13.7°$ and 23.0° [62, 63]. It is evident that as the composition of NH$_4$NO$_3$ is increased, the hump became more broaden and shifted to the higher angle indicating that the complexation has occurred between biopolymer host and ionic dopant. This observation revealed that the decrement of the crystalline phase in alginate occurs upon the addition of NH$_4$NO$_3$ which suggests that the amorphous phase has taken place in the SBE system. The amorphous phase contributes towards the increment of protonation of (H$^+$) in alginate and consequently improves the conductivity of the present system.

The analysis based on the crystallite size (D) in the present SBE system was carried out by using Eq. (1) to further investigate the effect of the addition of NH$_4$NO$_3$ in alginate. The full width at half maximum (FWHM) for each crystal peak/amorphous halo was observed and calculated using the PDXL software. The lists of crystallite size (D) for of alginate–NH$_4$NO$_3$ SBE system are tabulated in Table 4. It can be seen that the crystallite size of alginate decreases with the introduction of NH$_4$NO$_3$ and the sample that contains 25 wt.% of NH$_4$NO$_3$ (sample S5) exhibits only a single FWHM value which is also the lowest value of crystallinity in the present system. This finding indicates that only the amorphous phase

Table 3 Summary of complexation between alginate and NH$_4$NO$_3$ for the SBE system

Sample	Functional group with wavenumber (cm^{-1})					
	C–O–C bending	COO– stretching	NH$_4^+$ stretching	COO– stretching	NH$_4^+$ stretching	–OH stretching
S0	1019	1415	–	1598	–	3393
S1	1019	1412	1390	1598	–	3403
S2	1021	1410	1390	1604	–	3414
S3	1025	1410	1390	1604	3271	3426
S4	1028	1408	1390	1604	3271	3433
S5	1028	1406	1390	1605	3271	3442
S6	1028	–	1390	1605	3271	3448
S7	1028	–	1390	1605	3271	3452

was present. Previous studies [64–66] revealed that samples of polymer electrolytes with a lower crystallite size would exhibit high ionic conductivity, and hence, in the present system, it is expected that sample S5 possesses the highest ionic conductivity in SBE system.

It can be observed that the crystallinity behavior begins to appear between the ~ 14° and 40° region, in which the alginate was added more than 25 wt.% NH$_4$NO$_3$. The crystal peaks correspond to the appearance of NH$_4$NO$_3$ and alginate semi-crystalline phase. This implies that the alginate cannot solvate the NH$_4$NO$_3$ any longer due to the huge amount of H$^+$ concentration supplied to the SBE system that in turn blocks the ions migration. Consequently, the overcrowding of the ions led to the increase in crystallinity. The appearance of the crystalline peak also indicates that the deprotonation process has occurred as shown in the FTIR analysis. Based on XRD

results, it is expected that the transport properties and ionic conductivity in the present sample decreases.

Ionic conductivity analysis

The ionic conductivity of alginate–NH$_4$NO$_3$ SBE system at ambient temperature (303 K) is presented in Fig. 5. The ionic conductivity for the un-doped alginate SBE system was observed to be 2.94×10^{-7} S cm^{-1}, and with the addition of NH$_4$NO$_3$, the ionic conductivity began to increase towards a higher value. The dependence of the ionic conductivity on the NH$_4$NO$_3$ composition provides some insight into the specific interaction between the NH$_4$NO$_3$ and the alginate biopolymer matrix. The increase of the ionic conductivity in the alginate–NH$_4$NO$_3$ SBE system can be attributed to the ion association of proton H$^+$ as demonstrated in the FTIR study apart from the
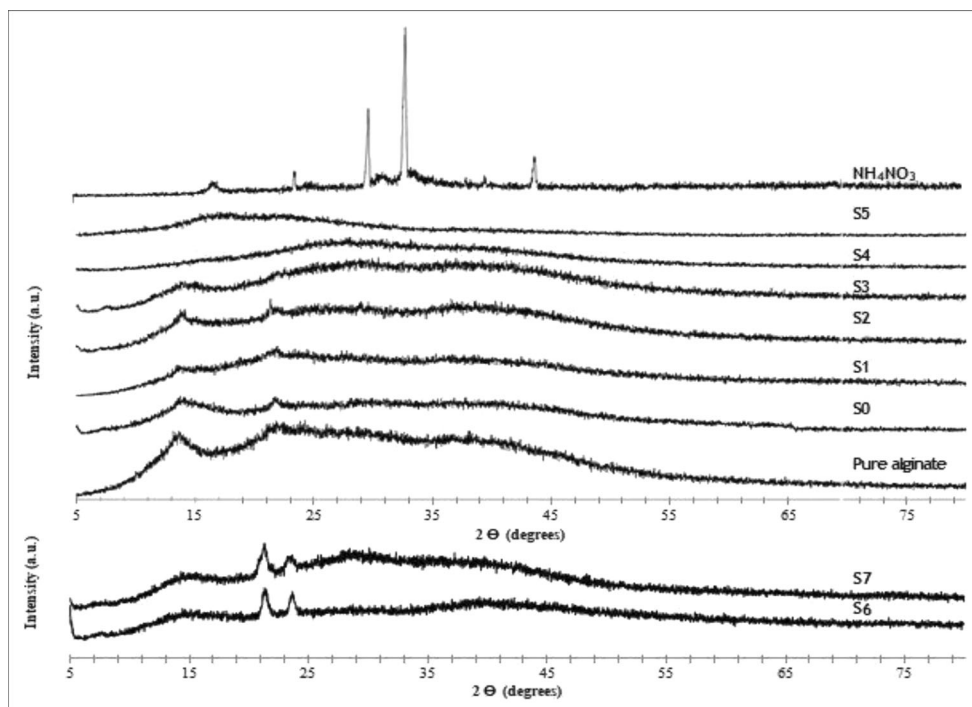

Fig. 4 XRD spectrum for the alginate–NH$_4$NO$_3$-based SBE system

Table 4 Crystallite size of the alginate–ammonium nitrate SBE system

Sample	2θ (degree)	FWHM (degree)	Crystallite size, D (Å)
S0	13.99	3.78	2.21
	21.75	0.83	10.18
	38.60	9.60	0.92
S1	14.46	4.09	2.04
	22.25	6.90	1.23
S2	13.64	1.90	4.40
	21.69	2.30	3.67
S3	13.72	3.02	2.77
	28.80	10.10	0.85
S4	28.13	8.10	1.05
S5	24.24	12.55	0.68
S6	14.46	5.01	1.67
	21.34	0.53	15.92
	23.61	0.48	17.65
	39.83	10.00	0.88
S7	15.21	2.96	2.83
	21.32	0.63	13.40
	28.20	5.60	1.53
	29.50	6.60	1.30

increment in transport properties [67–69]. In alginate–NH_4NO_3 SBE system, the ammonium salt will complex with the coordinating site (oxygen) of the alginate host. Hence, there will be more sites at which ion hopping and exchange can take place leading to an increase in conductivity. Moreover, XRD results also suggest that the increasing amorphous phase in the SBE system leads to an increase in the ionic conductivity.

The ionic conductivity achieved a maximum value at 5.56×10^{-5} S cm^{-1} for the sample containing 25 wt.% of NH_4NO_3 and this range of ionic conductivity value exhibited by the present system ($\sim 10^{-5}$ S/cm) is adequate enough to be applied as a supercapacitor [70] or EDLC [71] and proton battery [72] in electrochemical devices. However, it is worth noting that an increase of beyond 25 wt.% NH_4NO_3, the ionic
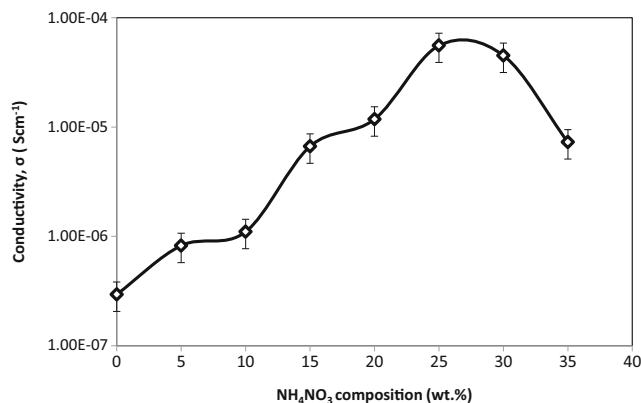

Fig. 5 Ionic conductivity of the alginate–NH_4NO_3 SBE system at ambient temperature

conductivity of SBE system starts to decrease, and the decrement in the ionic conductivity can be attributed to the re-association of the H$^+$ that changes into the neutral aggregation in ion cluster [73–75] as shown by FTIR result. In addition, the reason for such decrease in ionic conductivity may be due to the excess salt recrystallized out of the alginate as demonstrated by XRD result, which leads to an increase in the energy barrier to the segmental motion in the SBE system [76, 77].

Figure 6 presents the ionic conductivity at a different temperature range from 303 to 343 K for SBE system. Based on Fig. 6, it can be observed that the ionic conductivity increases gradually with temperature for all samples and the regression value, R^2 is observed to be close to unity ($R^2 \sim 1$) suggesting that all composition for alginate–NH_4NO_3 SBE system s are thermally activated and obey the Arrhenius behavior [78, 79]. This observation suggests that the ionic conductivity of the polymer electrolytes increases with temperature, and more often than not, it is commonly due to the increment in free volume in the present system allowing for the motion of the ions through the biopolymer backbone. Therefore, free volume around the biopolymer chain causes augmentation in mobility of ions and hence enhances the ionic conductivity with temperature. A similar result also has been reported with different types of polymer electrolyte system [52, 80, 81]. The Arrhenius relation can be expressed by

$$\sigma = \sigma_0 \exp\left(-\frac{E_a}{kT}\right) \tag{9}$$

where E_a is the activation energy, σ is the conductivity of SBE system, σ_0 is the pre-exponential factor, k is the Boltzmann constant, and T is the temperature.

The activation energy, E_a, values for alginate–NH_4NO_3 SBE system are plotted in Fig. 7. It can be observed that the value of E_a generally decreases as the ionic conductivity increases and evidently it is found to be the smallest E_a is demonstrated by the sample with the highest conductivity, i.e., at 25 wt.% of NH_4NO_3. This observation suggests that the ions which correspond to H$^+$ only requires lower energy to migrate to the coordinating sites (oxygen) in alginate and, in turn, enhances the ionic mobility. This is in agreement with the fact that the amount of ions in the SBE system increases with the increase in NH_4NO_3 composition, the energy barrier for the hopping decreases and leads to a decrease in the activation energy of the present system [78]. In addition, the low activation energy is due to the richness of amorphous phase in SBE system that facilitates a faster rate of H$^+$ ion motion in the biopolymer network [69, 75, 82, 83].

FTIR deconvolution

Figure 8 indicates the FTIR deconvolution of various samples of the SBE system. The region between 1500 and 1200 cm^{-1}

Fig. 6 Conductivity at different temperature of the alginate–NH_4NO_3 SBE system
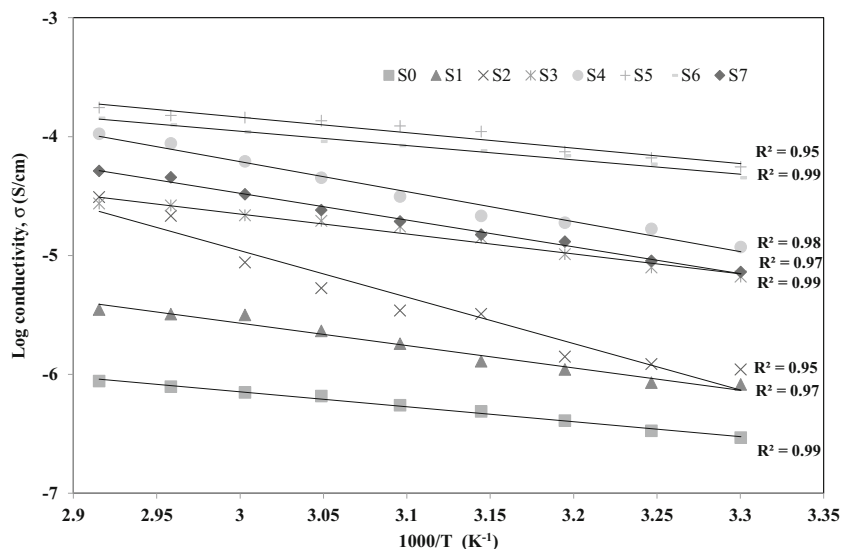
is selected as it is believed that complexation has occurred [84, 85] as observed in FTIR analysis. Based on Fig. 8, the free ions represent the free mobile ions (~ 1350 cm^{-1} to ~ 1400 cm^{-1}), and the contact ions pairs (~ 1420 cm^{-1} and ~ 1350 cm^{-1}) represent the contact ions and ion aggregates in the biopolymer system [35]. The free and contact ions were computed from the ratio of the area of free or contact ions to the total area of deconvolution peaks, respectively, and are tabulated in Table 5. The maximum ionic conductivity was observed is due to the maximum free ion formation as mentioned in the ionic conductivity analysis. This result supports the ionic conductivity observation in this SBE system.

It can be seen that the percentage of free ions increases as the composition of NH_4NO_3 is increased until sample S5 has similar conductivity pattern. The increase of free ions indicates that more H$^+$ is dissociated from NH_4^+ which would lead to an increase in ionic conductivity.

Based on Table 5, the number of ions, η, mobility of ions, μ, and diffusion coefficient, D, were calculated using Eqs. (4),

(5), and (6) and are presented in Fig. 9. From Fig. 9, it is apparent that the numbers of ions (η) increases gradually with the increase of NH_4NO_3, meanwhile the mobility of ions (μ) and the diffusion coefficient (D) are found to be aligned with the ionic conductivity pattern. It can be noted here that the increasing η values increase the ionic conductivity of the present system and this can be shown from the free ions values, which gradually increases with the addition of NH_4NO_3 to the SBE system. As the sample becomes more amorphous, H$^+$ migrates and interacts with COO$^-$ of alginate more efficiently, enhancing the ionic conductivity along with transport properties until the optimum value is reached.

However, beyond 25 wt.% NH_4NO_3, it was shown that the η value drastically increases to a higher value and meanwhile the μ and D are found to drop. This observation reveals that the present system is over-filled with huge concentration of ions (H$^+$) and in order to hop towards COO$^-$, it requires a huge amount of activation energy, which reflects towards the mobility and diffusion rate to drop [86, 87]. Besides, the appearance

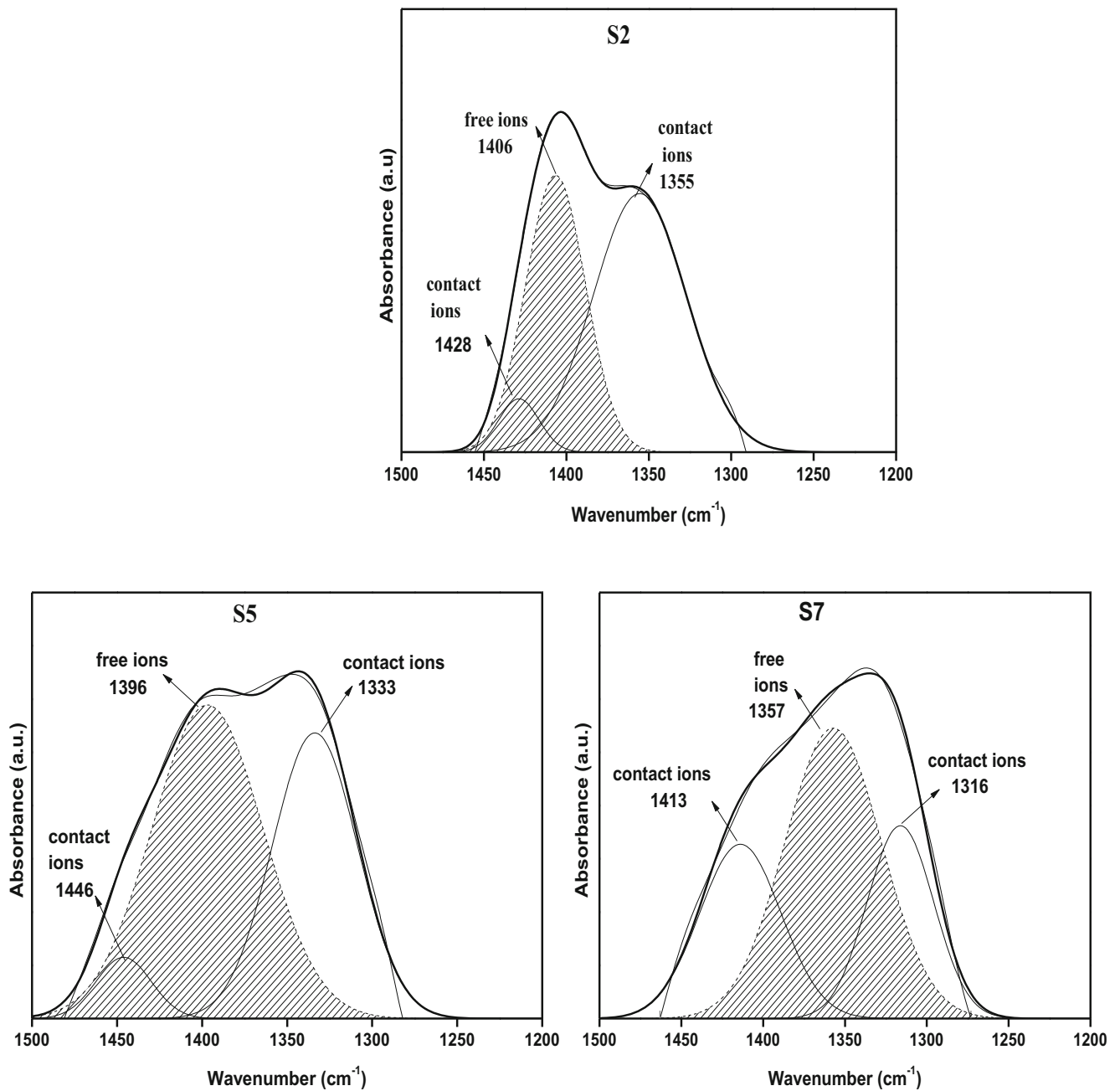**Fig. 7** Activation energy for the alginate–NH_4NO_3 SBE system
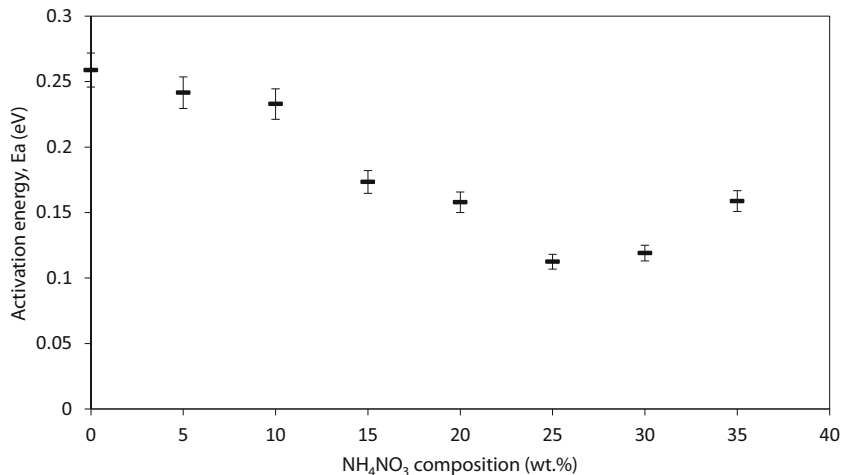
Fig. 8 FTIR deconvolution for various sample of the SBE system

Table 5 Percentage area of free and contact ions of the alginate–NH$_4$NO$_3$ SBE system

Sample	Free ion (%)	Contact ions (%)
S1	33.39	66.61
S2	38.77	61.23
S3	45.78	54.22
S4	50.67	49.33
S5	55.68	44.32
S6	51.06	48.94
S7	50.95	49.05

of the crystallinity peak for samples S6 and S7 as shown in the XRD analysis suggests that the pathway for ions hopping are limited. This is due to the blocking pathway for the transition of ions created by crystalline phase in the SBE system, consequently decreasing their mobility, diffusion, and ionic conductivity. This behavior is found to be in agreement with other research works on polymer electrolyte system [55, 66, 88].

Transference number measurement study

The transference number measurement is carried out to determine the conduction species (either cations or anions) in polymer

Fig. 9 Transport parameters of the alginate–NH$_4$NO$_3$ SBE system
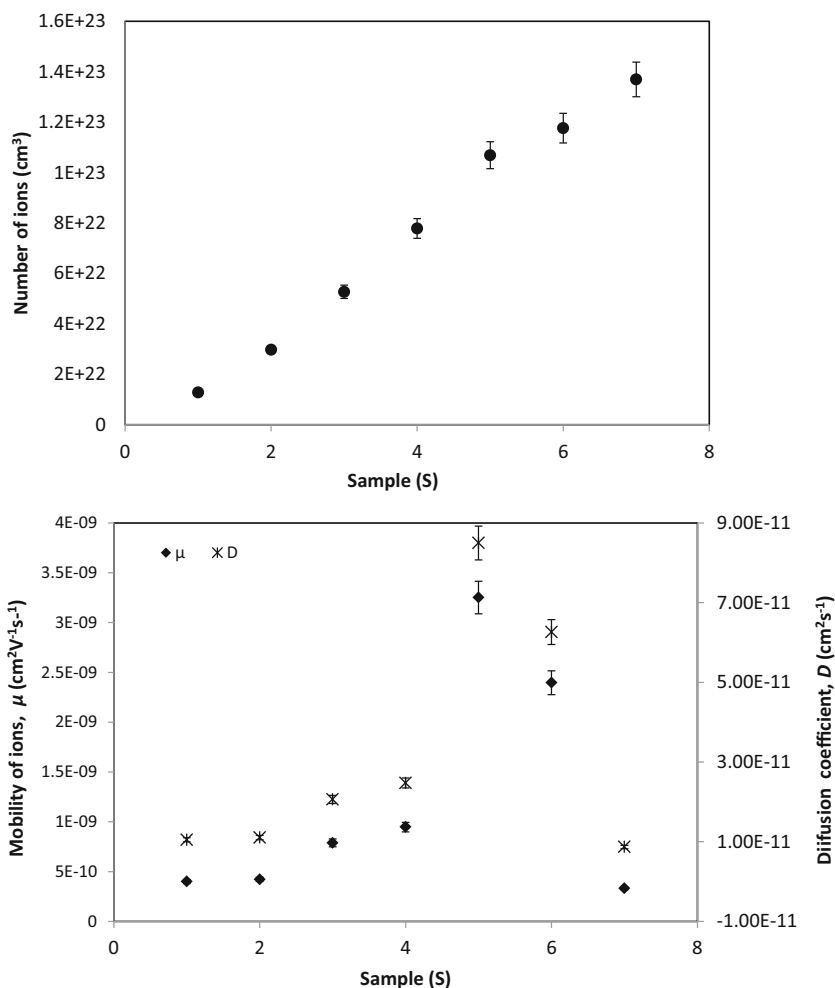
electrolyte system. The plots of normal polarized current versus time of the highest conducting sample in SBE system are illustrated in Fig. 10. The plots indicate that the initial total current, (I_i) decreased along the time and became plateau in the fully depleted state. The reason for the decrease of the ionic current is due to the
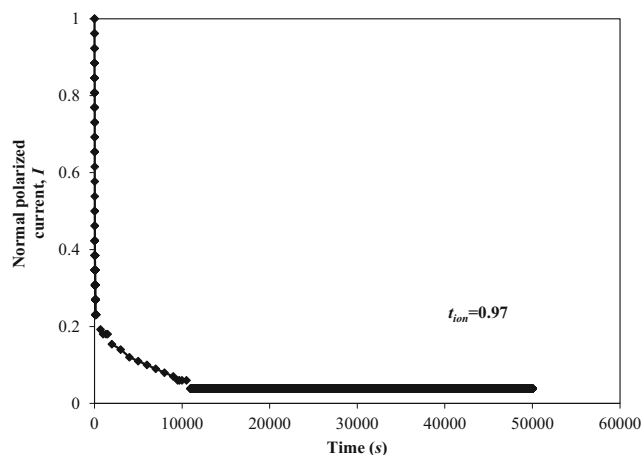

Fig. 10 The normal polarized current versus time for sample S5

reduction of the ionic conduction of the sample of alginate–NH$_4$NO$_3$. At steady state, the polarization occurred with current flows along the cell due to the presence of electrons across the electrolyte and the interfaces. One of the reasons for the ionic current to fall rapidly in an ion-blocking electrode is because the electrolyte is a cation. The ionic transference number and electron transference number of the highest in ionic conductivity were found to be 0.97 and 0.03, respectively. Thus, it can be inferred that the sample is dominantly due to the ions (H$^+$) from NH$_4$NO$_3$ complexed with alginate SBEs which are expected to be proton as the value of $t_{ion} \sim 1$ and this observation is also found to be in agreement with other similar works [89–91].

Differential scanning calorimetry analysis

Transport properties are affected by the presence of H$^+$ in the amorphous phase, which is characterized by the glass transition temperature (T_g) [92]. Figure 11 shows a typical plot of the DSC curves for the un-doped alginate and the highest conducting sample (25 wt.% NH$_4$NO$_3$) which has been recorded on the heating run temperature ranging from 30 to
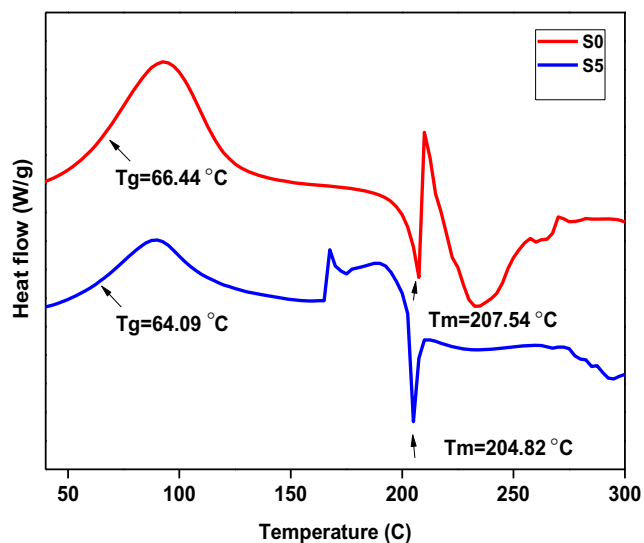
Fig. 11 DSC curves of pure alginate and 25 wt.% of NH_4NO_3

300 °C. It can be observed that the glass transition temperature, T_g, of pure alginate is 66.44 °C and this value is observed to be similar to the literature [93, 94]. Meanwhile, the T_g of alginate doped with 25 wt.% of NH_4NO_3 is found to be 64.09 °C, and the decrease in the T_g value may be attributed by the presence of NH_4NO_3 that increases the dissociation of H^+ from NH_4NO_3 for migration. With the increment of the amorphous phase in SBE system, the inhabitation of ionic motion to occur is also increased due to the increase in ionic coordination at the biopolymer host, that in turn, decreases the T_g value and raises the ionic conductivity of present system to a higher value [95–97]. Other researchers [98] have also reported the decrease in transition temperature as similarly reported in this work. In addition, the melting peak, T_m appears at 204.90 °C (S0) and 205.59 °C (S5), respectively. The value of T_m is observed to not to shift significantly; this is possibly be due to the physical entanglement of alginate polymer chains which limits the segmental motion of alginate [95].

Conclusion

In the present work, solid biopolymer electrolyte (SBE) system based on alginate doped with NH_4NO_3 was successfully prepared via solution-casting technique. The prepared samples were characterized using several techniques, namely, Fourier transform infrared (FTIR) spectroscopy, X-ray diffraction (XRD) and electrical impedance spectroscopy (EIS), transference number measurement (TNM) and differential scanning calorimetry (DSC). The complexation between alginate and NH_4NO_3 was established based on the changes of the peak which is observed from the coordinating site in alginate (COO^-, C–O–C, and –OH). The H^+ which originate from an N-H_4^+ group of NH_4NO_3 is believed to act as conducting

ions in the present system and lead to the increment in the amorphous phase as shown from the XRD results. The ionic conductivity of SBE system was found to increase from 2.94×10^{-7} and attained the highest ionic conductivity of 5.56×10^{-5} S cm^{-1} at ambient temperature for the sample containing with 25 wt.% NH_4NO_3. The temperature dependence observed in the present system indicates that the SBE system follows the Arrhenius behavior and is thermally activated. The calculated activation energy was found to be inversely proportional with ionic conductivity of SBE system, and sample S5 only requires a small amount of energy for ion migration. Based on the deconvolution method, the transport properties were calculated and revealed that the ionic conductivity of SBE system is governed by the mobility of ions and diffusion coefficient rate. Moreover, from the TNM analysis, it could be observed that the sample with the highest conductivity has a transference number t_{ion} of 0.97 suggesting that the conductivity is cation driven. Furthermore, the DSC analysis indicates that the decrease in the glass transition temperature (T_g) is correlated with the increase of the NH_4NO_3 composition in the present system.

References

1. Shuhaimi NEA, Alias NA, Kufian MZ, Majid SR, Arof AK (2010) Characteristics of methyl cellulose-NH_4NO_3-PEG electrolyte and application in fuel cells. J Solid State Electrochem 14:2153–2159
2. Agrawal RC, Hashmi SA, Pandey GP (2007) Electrochemical cell performance studies on all-solid-state battery using nano-composite polymer electrolyte membrane. Ionics 13:295–298
3. Sudhakar YN, Selvakumar M, Bhat DK (2013) LiClO$_4$-doped plasticized chitosan and poly(ethylene glycol) blend as biodegradable polymer electrolyte for supercapacitors. Ionics 19:277–285
4. Siebert E, Rosini S, Bouchet R, Vitter G (2003) Mixed potential type hydrogen sensor. Ionics 9:168–175
5. Singh R, Bhattacharya B, Gupta M, Khan ZH, Tomar SK, Singh V, Singh PK (2017) Electrical and structural properties of ionic liquid doped polymer gel electrolyte for dual energy storage devices. Int J Hydrog Energy 42:14602–14607
6. Deepa M, Sharma N, Agnihotry SA, Singh S, Lal T, Chandra R (2002) Conductivity and viscosity of liquid and gel electrolytes based on LiClO$_4$, LiN(CF$_3$SO$_2$)$_2$ and PMMA. Solid State Ionics 152–153:253–258
7. Perera K, Dissanayake MAKL (2006) Conductivity variation of the liquid electrolyte, EC: PC: LiCF$_3$SO$_3$ with salt concentration. Sri Lankan J Phys 7:1–5
8. Zhao D, Fei Z, Ang WH, Dyson PJ (2007) Sulfonium-based ionic liquids incorporating the allyl functionality. Int J Mol Sci 8:304–315

9. Muthupradeepa R, Sivakumar M, Subadevi R, Suryanarayanan V (2017) Sulfonium cation based ionic liquid incorporated polymer electrolyte for lithium ion battery. Polym Bull 74:1677–1691

10. Fisher AS, Khalid MB, Widstrom M, Kofinas P (2011) Solid polymer electrolytes with sulfur based ionic liquid for lithium batteries. J Power Sources 196:9767–9773

11. Kim HJ, Boysen DA, Newhouse JM, Spatocco BL, Chung B, Burke PJ, Bradwell DJ, Jiang K, Tomaszowska AA, Wang K, Wei WF, Ortiz LA, Barriga SA, Poizeau SM, Sadoway DR (2013) Liquid metal batteries: past, present, and future. Chem Rev 113:2075–2099

12. Ahmad Z, Isa MIN (2012) Ionics Conduction via Correlated Barrier Hoping Mechanism in CMC-SA Solid Biopolymer Electrolytes. Int J Latest Res Sci Technol 2:70–75

13. Ahmad NH, Isa MIN (2015) Structural and Ionic Conductivity Studies of CMC Based Polymer Electrolyte Doped with NH_4Cl. Adv Mater Res 1107:247–252

14. Shukur MF, Kadir MFZ (2015) Hydrogen Ion Conducting Starch-Chitosan Based Electrolyte for Application in Electrochemical Devices. Elecrochim Acta 158:152–165

15. Nithya S, Selvasekarapandian S, Karthikeyan S, Inbavalli D, Sikkinthar S, Sanjeeviraja C (2014) AC impedance studies on proton-conducting PAN: NH_4SCN polymer electrolytes. Ionics 20:1391–1398

16. Khanmirzaei MH, Ramesh S (2014) Studies on biodegradable polymer electrolyte rice starch (RS) complexed with lithium oxide. Ionics 20:691–695

17. Majid SR, Idris NH, Hassan MF, Winnie T, Khiar ASA, Arof AK (2005) Transport studies on filler-doped chitosan based polymer electrolyte. Ionics 11:451–455

18. Machado GO, Ferreira H, Pawlicka A (2005) Influence of plasticizer contents on the properties of HEC-based solid polymeric electrolytes. Electrochim Acta 50:3827–3833

19. Singh R, Bhattacharya B, Tomar SK, Singh V, Singh PK (2017) Electrical, optical and electrophotochemical studies on agarose based biopolymer electrolyte towards dye sensitized solar cell application. Measurement 102:214–219

20. Singh R, Singh PK, Singh V, Bhattacharya B (2017) Agarose Biopolymer Electrolytes: Ion Conduction Mechanism and Dielectric Studies. Cellul Chem Technol 51:949–955

21. Guarino V, Caputo T, Altobelli R, Ambrosio L (2015) Degradation properties and metabolic activity of alginate and chitosan polyelectrolytes for drug delivery and tissue engineering applications. AIMS Mater Sci 2:497–502

22. Kanasan N, Adzila S, Azimah MN, Gurubaran P (2017) The Effect of Sodium Alginate on the Properties of Hydroxyapatite. Procedia Eng 184:442–448

23. Varshney PK, Gupta S (2011) Natural polymer-based electrolytes for electrochemical devices: a review. Ionics 17:479–483

24. Papageorgiou SK, Kouvelos EP, Favvas EP, Sapalidis AA, Romanos GE, Katsaros FK (2010) Metal–carboxylate interactions in metal–alginate complexes studied with FTIR spectroscopy. Carbohydr Res 345:469–473

25. Obot IB, Onyeachu IB, Kumar AM (2017) Sodium alginate: A promising biopolymer for corrosion protection of API X60 high strength carbon steel in saline medium. Carbohydr Polym 178:200–208

26. Kosik A, Luchowska U, Święszkowski W (2016) Electrolyte alginate/poly-l-lysine membranes for connective tissue development. Mater Lett 184:104–107

27. Florea MG, Nedelcu IA, Ungureanu C, Ficai A, Ficai D, Guran C, Andronescu E (2013) Alginate and sulfanilamide based DDS with antibacterial activity. Int J Polym Mater Polym Biomater 63:92–96

28. Liang Li LW, Yang S, Rui N, Tingting Z, Shirui M (2013) Drug release characteristics from chitosan–alginate matrix tablets based on the theory of self-assembled film. Int J Pharm 450:197–207

29. Rahaman MHA, Khandaker MU, Khan ZR, Kufian MZ, Noor IM, Arof AK (2014) Effect of gamma irradiation on poly(vinyledene difluoride)-lithium bis(oxalato) borate electrolyte. Phys Chem Chem Phys 16:11537–11157

30. Sim LN, Arof AK (2017) Elastomers and their potential as matrices in polymer electrolytes. Intech 10:5772–5809

31. Lalitha S, Sathyamoorthy R, Senthilarasu S, Subbarayan A, Natarajan K (2004) Characterization of CdTe thin film—dependence of structural and optical properties on temperature and thickness. Sol Energy Mater Sol Cells 82:187–199

32. Sawaby A, Selim MS, Marzouk SY, Mostafa MA, Hosny A (2010) Structure, optical and electrochromic properties of NiO thin films. Physica B: Condensed Matter 405:3412–3420

33. Chai MN, Isa MIN (2016) Novel Proton Conducting Solid BioPolymer Electrolytes based on Carboxymethyl Cellulose Doped with Oleic Acid and Plasticized with Glycerol. Sci Rep 6:27328–27334

34. Zainuddin NK, Samsudin AS (2018) Investigation on the Effect of NH_4Br at Transport Properties in K–Carrageenan Based Biopolymer Electrolytes via Structural and Electrical Analysis. Mater Today Commun 14:199–209

35. Ramli MA, Isa MIN (2016) Structural and ionic transport properties of protonic conducting solid biopolymer electrolytes based on carboxymethyl cellulose doped ammonium fluoride. J Phys Chem B 120:11567–11573

36. Rasali NMJ, Samsudin AS (2017) Ionic transport properties of protonic conducting solid biopolymer electrolytes based on enhanced carboxymethyl cellulose - NH_4Br with glycerol. Ionics 1-12

37. Arof AK, Amirudin S, Yusuf SZ, Noor IM (2014) A method based on impedance spectroscopy to determine transport properties of polymer electrolytes. Phys Chem Chem Phys 16:1856–1867

38. Nik Aziz NA, Idris NK, Isa MIN (2010) Proton conducting polymer electrolytes of methylcellulose doped ammonium fluoride: Conductivity and ionic transport studies. Int J Phys Sci 5:748–752

39. Ahmad NHB, Isa MIN (2015) Proton conducting solid polymer electrolytes based carboxymethyl cellulose doped ammonium chloride: ionic conductivity and transport studies. Int J Plast Technol 19:47–55

40. Samsudin AS, Lai HM, Isa MIN (2014) Biopolymer materials based carboxymethyl cellulose as a proton conducting biopolymer electrolyte for application in rechargeable proton battery. Electrochim Acta 129:1–13

41. Chen W, Feng Q, Zhang G, Yang Q, Zhang C (2017) The effect of sodium alginate on the flotation separation of scheelite from calcite and fluorite. Miner Eng 113:1–7

42. Helmiyati, Aprilliza M (2017) Characterization and properties of sodium alginate from brown algae used as an ecofriendly superabsorbent. IOP Conf Ser Mater Sci Eng 188:12019

43. Kanti P, Srigowri K, Madhuri J, Smitha B, Sridhar S (2004) Dehydration of ethanol through blend membranes of chitosan and sodium alginate by pervaporation. Sep Purif Technol 40:259–266

44. Himanshu KS, Dushyant AS (2016) Formulation Optimization and Evaluation of Probiotic Lactobacillus sporogenes -Loaded Sodium Alginate with Carboxymethyl Cellulose Mucoadhesive Beads Using Design Expert. J Food Process 2016:1–14

45. Li P, Dai YN, Zhang JP, Wang AQ, Wei Q (2008) Chitosan–alginate nanoparticles as a novel drug delivery system for nifedipine. Int J Biomed Sci 4:221–228

46. Bourahla S, Ali Benamara A, Kouadri Moustefai S (2014) Infrared spectra of inorganic aerosols: ab initio study of $(NH_4)_2SO_4$, NH_4NO_3, and $NaNO_3$. Can J Phys 92:216–221

47. Shuhaimi NEA, Majid SR, Arof AK (2009) On complexation between methyl cellulose and ammonium nitrate. Mater Res Innov 13:239–242

48. Hong BW, Man NC, Chak KC (2007) FTIR Characterization of Polymorphic Transformation of Ammonium Nitrate. Aerosol Sci Technol 41:581–588

49. Sohaimy MIH, Isa MIN (2017) Ionic conductivity and conduction mechanism studies on cellulose based solid polymer electrolytes doped with ammonium carbonate. Polym Bull 74:1371–1386

50. Samsudin AS, Khairul WM, Isa MIN (2012) Characterization on the potential of carboxy methylcellulose for application as proton conducting biopolymer electrolytes. J Non-Cryst Solids 358:1104–1112

51. Ilie A, Ghiţulică C, Andronescu E, Cucuruz A, Ficai A (2016) New composite materials based on alginate and hydroxyapatite as potential carriers for ascorbic acid. Int J Pharm 510:501–507

52. Hashmi SA, Kumar A, Maurya KK, Chandra S (1990) Proton-conducting polymer electrolyte.I. The polyethylene oxide+ NH_4ClO_4 system. J Phys D: Appl Phys 23:1307–1314

53. Mason RN, Hu L, Glatzhofer DT, Frech (2010) Infrared spectroscopic and conductivity studies of poly (N-methylpropylenimine)/ lithium triflate electrolytes. Solid State Ionics 180:1626–1632

54. Kadir MF, Aspanut Z, Majid SR, Arof AK (2011) FTIR studies of plasticized poly (vinyl alcohol)–chitosan blend doped with NH_4NO_3 polymer electrolyte membrane. Spectrochim Acta A 78:1068–1074

55. Samsudin AS, Isa MIN (2012) Structural and ionic transport study on CMC doped NH_4Br: A new types of Biopolymer Electrolytes. J Appl Sci 12:174–179

56. Chai MN, Isa MIN (2013) The oleic acid composition effect on the carboxymethyl cellulose based biopolymer electrolyte. J Crystallization Process Technol 3:1–4

57. Kamarudin KH, Isa MIN (2013) Structural and DC Ionic conductivity studies of carboxy methylcellulose doped with ammonium nitrate as solid polymer electrolytes. Int J Phys Sci 8:1581–1587

58. Bitner-Michalska A, Nolis GM, Żukowska G, Zalewska A, Poterała M, Trzeciak T, Dranka M, Kalita M, Jankowski P, Niedzicki L, Zachara J (2017) Fluorine-free electrolytes for all-solid sodium-ion batteries based on percyano-substituted organic salts. Sci Rep 7:40036

59. Samsudin AS, Aziz MIA, Isa MIN (2012) Natural Polymer Electrolyte System Based on Sago: Structural and Transport Behavior Characteristics. Int J Polym Anal Ch 17:600–607

60. Hema M, Selvasekerapandian S, Sakunthala A, Arunkumar D, Nithya H (2008) Structural, vibrational and electrical characterization of PVA–NH_4Br polymer electrolyte system. Physica B 403:2740–2747

61. Shukur MF, Ithnin R, Kadir MFZ (2014) Protonic Transport Analysis of Starch-Chitosan Blend Based Electrolytes and Application in Electrochemical Device. Mol Cryst Liq Cryst 603:52–65

62. Wang Q, Hu X, Du Y, Kennedy JF (2010) Alginate/starch blend fibers and their properties for drug controlled release. Carbohydr Polym 82:842–847

63. Yang G, Zhang L, Peng T, Zhong W (2000) Effects of Ca^{2+} bridge cross-linking on structure and pervaporation of cellu-lose/alginate blend membranes. J Membr Sci 175:53–60

64. Samsudin AS, Isa MIN (2011) New types of biopolymer electrolytes: Ionic conductivity study on CMC doped with NH_4Br. Journal of Current Engineering Research 2:2250–2637

65. Balasubramanyam AV, Reddy TJR, Sharma AK, Narasimha Rao VVR (2007) Electrical, optical, and structural characterization of polymer blend (PVC/PMMA) electrolyte films. Ionics 13:349–354

66. Shuhaimi NEA, Teo LP, Majid SR, Arof AK (2010) Transport studies of NH_4NO_3 doped methyl cellulose electrolyte. Synthetic Met 160:1040–1044

67. Ramlli MA, Kamarudin KH, Isa MIN (2015) Ionic Conductivity and Structural Analysis of Carboxymethyl Cellulose Doped With Ammonium Fluoride as Solid Biopolymer Electrolytes. Am Eurasian J Sustain. Agric 9:46–51

68. Nik Aziz NA, Isa MIN (2012) FTIR and electrical studies of methylcellulose doped NH_4F solid polymer electrolytes. Solid State Sci Tech Letters 19:37–47

69. Selvasekarapandian S, Hirankumar G, Kawamura J, Kuwata N, Hatton T (2005) ^1H solid state NMR studies on the proton conducting polymer electrolytes. Mater Lett 59:2741–2745

70. Suriani AB, Nurhafizah MD, Mohamed A, Zainol I, Masrom AK (2015) A facile one-step method for graphene oxide/natural rubber latex nanocomposite production for supercapacitor applications. Mat Lett 161:665–668

71. Francis KA, Liew CW, Ramesh S (2016) Effect of ionic liquid 1-butyl-3-methylimidazolium bromide on ionic conductivity of poly (ethyl methacrylate) based polymer electrolytes. Mater Express 6:252–258

72. Shukur MF, Ithnin R, Illias HA, Kadir MF (2013) Proton conducting polymer electrolyte based on plasticized chitosan–PEO blend and application in electrochemical devices. Opt Mater 35:1834–1841

73. Prasanth R, Aravindan V, Srinivasan M (2012) Novel polymer electrolyte based on cob-web electrospun multi component polymer blend of polyacrylonitrile/poly(methyl methacrylate)/ polystyrene for lithium ion batteries-Preparation and electrochemical characterization. J Power Sources 202:299–307

74. Hodge RM, Edward GH, Simon GP (1996) Water Absorption and States of Water in Semicrystalline Poly (Vinyl Alcohol) Films. Polymer 37:1371–1376

75. Schantz S, Torell LM (1993) Evidence of dissolved ions and ion pairs in dilute poly (propylene oxide)-salt solutions. Solid State Ionics 60:47–53

76. Teeters D, Neuman R, Tate BD (1996) The concentration behavior of lithium triflate at the surface of polymer electrolyte materials. Solid State Ionics 85:239–245

77. Othman MFM, Samsudin AS, Isa MIN (2012) Ionic conductivity and relaxation process in CMC-G.A solid biopolymer electrolytes. J Current Eng Res 2:6–10

78. Rajendran S, Uma T (2000) Experimental investigations on PVC–$LiAsF_6$–DBP polymer electrolyte systems. J Power Sources 87:218–222

79. Sit YK, Samsudin AS, Isa MIN (2012) Ionic Conductivity Study on Hydroxyethyl Cellulose (HEC) doped with NH_4Br Based Biopolymer Electrolytes. Res J Recent Sci 1:16–21

80. Khiar ASA, Arof AK (2010) Conductivity studies of starch-based polymer electrolytes. Ionics 16:123–129

81. Buraidah MH, Teo LP, Majid SR, Arof AK (2009) Ionic conductivity by correlated barrier hopping in NH_4I doped chitosan solid electrolyte. Physica B 404:1373–1379

82. Srivastava N, Chandra S (2000) Studies on a new proton conducting polymer system: poly(ethylene succinate) + NH_4ClO_4. Eur Polym J 36:421–433

83. Kopitzke RW, Linkous CA, Anderson HR, Nelson GL (2000) Conductivity and water uptake of aromatic-based proton exchange membrane electrolytes. J Electrochem Soc 147:1677–1681

84. Hema M, Selvasekarapandian S, Hirankumar G, Sakunthala A, Arunkumar D, Nithya H (2010) Laser Raman and ac impedance spectroscopic studies of PVA: NH_4NO_3 polymer electrolyte. Spectrochim Acta 75:474–478

85. Selvasekarapandian S, Hema M, Kawamura J, Kamishima O, Baskaran R (2010) Characterization of PVA–NH_4NO_3 polymer electrolyte and its application in rechargeable proton battery. J Phys Soc Jpn 79:163–168

86. Ramesh S, Ng KY (2009) Characterization of polymer electrolytes based on high molecular weight PVC and Li_2SO_4. Curr Appl Phys 9:329–332

87. Chai MN, Ramlli MA, Isa MIN (2013) Proton conductor of pro-pylene carbonate–plasticized carboxyl methylcellulose–based solid polymer electrolyte. Int J Polym Anal Charact 18:297–302

88. Samsudin AS, Kuan ECH, Isa MIN (2011) Investigation of the potential of proton conducting biopolymer electrolytes based methyl cellulose-glycolic acid. Int J Polym Anal Charact 16:477–485

89. Selvalakshmi S, Vijaya N, Selvasekarapandian S, Premalatha M (2017) Biopolymer agar-agar doped with NH_4SCN as solid polymer electrolyte for electrochemical cell application. J Appl Polym Sci 134

90. Biswal DR, Singh RP (2004) Characterisation of Carboxymethyl Cellulose and Polycrylamide graft copolymer. Carbohydr Polym 57:379–387

91. Muthuvinayagam M, Gopinathan C (2015) Characterization of proton conducting polymer blend electrolytes based on PVdF-PVA. Polymer 68:122–130

92. Saikia D, Pan YC, Kao HM (2012) Synthesis, multinuclear NMR characterization and dynamic property of organic–inorganic hybrid electrolyte membrane based on alkoxysilane and poly(oxyalkylene) diamine. Membranes 2:253–274

93. Swamy TM, Ramaraj B, Lee JH (2008) Sodium alginate and its blends with starch: thermal and morphological properties. J Appl Polym Sci 109:4075–4081

94. Swamy TM, Ramaraj B, Siddaramaiah (2010) Sodium alginate and poly (ethylene glycol) blends: thermal and morphological behaviors. J Macromol Sci A 47:877–881

95. Matkovska L, Iurzhenko M, Mamunya Y, Tkachenko I, Demchenko V, Synyuk V, Boiteux G (2017) Structural Peculiarities of Ion-Conductive Organic-Inorganic Polymer Composites Based on Aliphatic Epoxy Resin and Salt of Lithium Perchlorate. Nanoscale Res Lett 12:423

96. Kobayashi N, Uchiyama M, Shigehara K, Tsuchida E (1985) Ionically high conductive solid electrolytes composed of graft co-polymer-lithium salt hybrids. J Phys Chem 89:987–991

97. Johan MR, Ting LM (2011) Structural, thermal and electrical properties of nano manganese-composite polymer electrolytes. Int J Electrochem Sci 6:4737–4748

98. Shukur MF, Ithnin R, Kadir MFZ (2014) Electrical properties of proton conducting solid biopolymer electrolytes based on starch–chitosan blend. Ionics 20:977–999